A Theoretical Study on the Reaction Mechanism for the Bergman Cyclization from the Perspective of the Electron Localization Function and Catastrophe Theory

Juan C. Santos,[†,‡] Juan Andres,[*,‡] Arie Aizman,[†] Patricio Fuentealba,[§] and Victor Polo[‡]

Departamento de Química, Universidad Técnica Federico Santa Maria, Casilla 110-V, Valparaíso, Chile, Departament de Ciències Experimentals, Universitat Jaume I, Apartat 224, 12080, Castelló, Spain, and Departamento de Física, Universidad de Chile, Las Palmeras 3425, Santiago, Chile

Received: December 21, 2004; In Final Form: February 21, 2005

The reaction mechanism associated with the Bergman cyclization of the (*Z*)-hexa-1,5-diyne-3-ene to render *p*-benzyne has been analyzed by means of a combined use of the electron localization function (ELF) and the catastrophe theory on the basis of density functional theory (DFT) calculations (B3LYP/6-31G(d)). The complex electronic rearrangements of this reaction can be highlighted using this novel quantum mechanical perspective. Five domains of structural stability of the ELF occurring along the intrinsic reaction path as well as four catastrophes (fold-cusp-fold-cusp) responsible for the changes in the topology of the system have been identified. The multiple factors that occur along the intrinsic reaction coordinate path are presented and discussed in a consistent way. The topological analysis of ELF and catastrophe theory reveals that mechanical deformation of the $C_1-C_2-C_3$ unit and closed-shell repulsion between terminal acetylene groups lead to an early formation of diradicaloid character at C_2 and C_5 atoms. Immediately after the transition structure (TS) is reached, the open-shell-singlet biradical becomes stable. Meanwhile, C_1 and C_6 atoms are preparing to be covalently bonded; that will finally occur at a distance of 1.791 Å. In addition, a separation of the ELF into in-plane (σ) and out-of-plane (π) contributions allows us to discuss the aromaticity profiles; σ-aromaticity appears in the vicinities of the TS, while π-aromaticity takes place in the final stage of the reaction path, once the ring has been formed.

Introduction

Modern computational schemes offer the possibility of an accurate relationship between the concepts of chemistry and the properties of molecular wave functions. In this sense, the rules, models, and explanations that the chemical community has used over the years can be sustained from physical grounds. In recent times, the electron localization function (ELF, $\eta(\mathbf{r})$) of Becke and Edgecombe,[1] which provides an orbital independent description of the electron localization based on strong physical arguments regarding the Fermi hole,[2,3] has received considerable attention. The ELF is defined (eq 1) in terms of the excess of local kinetic energy density due to the Pauli exclusion principle, $T(\rho(\mathbf{r}))$, and the Thomas−Fermi kinetic energy density, $T_h(\rho(\mathbf{r}))$:

$$\mathrm{ELF} = \left[1 + \left(\frac{T(\rho(\mathbf{r}))}{T_h(\rho(\mathbf{r}))}\right)^2\right]^{-1} \qquad (1)$$

Its numerical values are conveniently mapped on the interval (0,1) facilitating its analysis. According to the interpretation of the ELF, a region of the space with a high value of ELF corresponds to a region where it is more probable to localize an electron or a pair of electrons. The topological analysis of the ELF gradient field, $\nabla\eta(\mathbf{r})$, provides a mathematical model enabling the partition of the molecular position space in a set of continuous and nonoverlapping basins of attractors that present in principle a one-to-one correspondence with electron pairs. In this way, an accurate calculation of chemical local objects such as bonds, lone pairs, or atomic shells can be achieved.[4] The basins are either core basins labeled C(A) or valence basins V(A,...) belonging to the outermost shell. Valence basins are characterized by their coordination number (the synaptic order) with core. This method has been well documented in a series of articles presenting its theoretical foundations.[1,4−10] The original work of Silvi and Savin[4−6] on the ELF generated a fruitful field of applications in a variety of chemical problems, ranging from structural[11,12] and chemical reactivity studies,[13−20] as well as the study of chemical reactions in terms of elementary catastrophes.[21−27] Very recently, Silvi[10] has defined the size-independent spin-pair composition function, which possesses a clear meaning as a local indicator of chemical bonding.

Recently, a combination of ELF and catastrophe theory of R. Thom[28] has been employed to analyze the molecular changes occurring along the reaction path for the molecular mechanism of the Diels−Alder reaction between 1,3-butadiene and ethylene,[26] and the 1,3 dipolar cycloaddition between fulminic acid and acetylene.[27] The study of the evolution of ELF basins along the reaction path enables one to identify the turning points where there is a change in the number or type of ELF basins. Because ELF depends on the electron density, it does not provide separate information about in-plane (σ) and out-of-plane (π) delocalizations in a molecule. A separation of the ELF into its σ and π contributions was shown to provide a useful scheme to discuss the aromatic character in a molecular system.[29,30] This approach uses the fact that the kinetic energy is additive and it can be

* Corresponding author. Phone: (+34) 964-728071. Fax: (+34) 964-728066. E-mail: andres@exp.uji.es.
[†] Universidad Técnica Federico Santa Maria.
[‡] Universitat Jaume I.
[§] Universidad de Chile.

10.1021/jp0441947 CCC: $30.25
Published on Web 04/02/2005

SCHEME 1: The Bergman Cyclization of (*Z*)-Hexa-1,5-diyne-3-ene

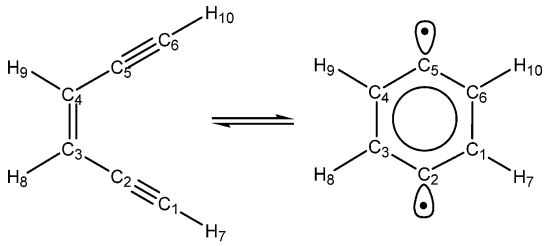

decomposed into σ (ELF_σ) and π (ELF_π) parts. Very recently, it has been shown that the analysis of the averaged values of ELF_σ and ELF_π can be considered as an appropriate measure of the net aromaticity of different molecular systems.[30] In other work, Melin and Fuentealba[31] have shown that a suitable separation of the ELF between α-spin and β-spin parts yields a reasonable description of the localization of the spin density.

The Bergman reaction[32] provides an example of cycloaromatization leading to the formation of 1,4 dehydrobenzene (*p*-benzyne) biradical (see Scheme 1) along a complex reorganization of formally triple, double, and single carbon−carbon bonds. This is a paradigmatic example because the nature of the electronic effects involves simultaneous but differently timed changes in two orthogonal π-systems. In addition, the product, *p*-benzyne, plays a key role in different steps with potential chemistry and biological activity.[33,34] Given their relevance, a large number of studies have been devoted to understanding this class of chemical reactions.[35−54] In particular, the question of the in-plane and out-of-plane interactions in the cyclization of (*Z*)-hexa-1,5-diyn-3-ene has been the subject of detailed theoretical studies in recent years.[48,53,54] Galbraith and co-workers[48] using valence bond (VB) arguments analyze the progression of changes in the in-plane and out-of-plane systems, concluding that changes in the in-plane orbitals occur much earlier in the intrinsic reaction coordinate (IRC) path, controlling the energy activation of the cyclization; a similar conclusion is obtained using multiconfigurational calculations by Gleiter and Haberhauer.[46] Another study from Stahl and co-workers,[53] using thermodynamic arguments and detailed nucleus-independent chemical shift (NICS) calculations, suggests some contribution of the π-system to the total NICS at the transition structure. Following seminal analysis of Koga and Morokuma,[35] Alabugin and Manoharan[54] have recently carried out a theoretical work using natural bond analysis (NBO) along the IRC path, concluding that the interplay between attractive and repulsive forces in the in-plane π-system controls the energy barrier.

Several factors are involved in different stages of the electronic rearrangement that leads from (*Z*)-hexa-1,5-diyne-3-ene to *p*-benzyne. On the destabilizing side, one can cite the breaking of acetylenic bonds as a result of their bending, the closed-shell repulsion between terminal acetylenic groups, and the fact that, at a distance rC_1-C_6 of ca. 3 Å (near the Nicolaou's threshold[55]), the in-plane π orbitals become parallel and resemble the "antiaromatic" TS of the symmetry-forbidden $[2_s+2_s]$ cycloaddition, as pointed out by Alabugin et al.[54] On the other hand, inspection of *p*-benzyne reveals some stabilizing effects such as the ring closure by the formation of the C_1-C_6 bond, the presence of unpaired electrons on C_2, C_5, and the aromaticity of the out-of-plane electronic system. The motivation of the current work is to present and to discuss these factors and effects globally, paying special attention to the timing along the reaction path, from the novel perspective of the joint use of the ELF, catastrophe theory, and the assessment of aromaticity by taking into account ELF_σ and ELF_π contributions. The Article is arranged as follows. In the next section, we present the computational method as well as a brief summary of the background required for our theoretical study. In the third section, we discuss in detail the results obtained by our analysis, comparing them to previous results obtained by other studies. A short conclusion section closes the paper.

Theoretical Methods

The calculations were carried out by means of the DFT using the B3LYP hybrid exchange-correlation functional[56−58] with the 6-31G(d)[59] basis set as included in the Gaussian 98 program.[60] The B3LYP has proven to yield accuracy enough to provide a satisfactory description of the Bergman cyclization,[50] although reaction endothermicity is underestimated. Some authors[40,41,49] recommend employing pure functionals instead of the hybrid version to describe these type of reactions. The superiority of the BLYP over the more general B3LYP method is not clear and, in particular, the calculation of the reaction pathway, so we have chosen the B3LYP functional. Geometry optimizations for all of the stationary points considered here have been calculated. For each optimized stationary point, a vibrational analysis was performed to determine its character, all positive for a minimum and one imaginary for TS. The IRC method of Fukui[61,62] developed by Gonzalez and Schlegel[63] was employed to trace the reaction path in mass-weighted coordinates from reactants to products. The calculated reaction path comprises 266 points (including the stationary points) with a step size equal to 0.04 $amu^{1/2}$ bohr.

The stability of the wave function was checked in all points of the reaction pathway according to the procedure described by Bauernschmitt and Ahlrichs;[64] those points where the restricted (RDFT) wave function presented an instability were reoptimized using the unrestricted broken spin symmetry (BS-UDFT) description, whether the constrain $\psi_a = \psi_b$ is lifted.[41,49,65] In this way, the total IRC path is composed of two parts: the closed-shell (RB3LYP) from the reactive to the TS and the open-shell (BS-UB3LYP), which starts one point after the TS and concludes at the product. The Kohn−Sham orbitals were obtained for each point of the calculated IRC path, and the ELF analysis was carried out using a cubical grid of step size smaller than 0.1 Bohr employing the TopMod[66] package of programs. The graphical representation was obtained using the MOLEKEL program.[67]

As was previously pointed out, in the framework established by the ELF analysis, a chemical reaction is viewed as a series of topological changes occurring along the reaction path. Changes in the control parameters defining the reaction pathway (such as the nuclear coordinates and the electronic state) can lead to different configurations of the ELF topology. The evolution of the bonding along the reaction path is modeled by the changes in the number and synaptic orders of the ELF valence basins. Each topology configuration is only possible for values of the control parameters comprised into well definite ranges or, in other words, into subsets called structural stability domains or simply "steps". Two points of the control space belonging to the same step possess the same number of critical points of each type in the ELF gradient field.

Within a step, the critical points on the ELF scalar field (i.e., points at which $\nabla \eta(r) = 0.0$) are said to be hyperbolic; that is, all eigenvalues of the Hessian matrix are not zero. The turning points between two consecutive steps present at least one critical

TABLE 1: Integrated Electron Populations ($\bar{N}$) Calculated for Valence ELF Basins Involved in the Bergman Cyclization of (*Z*)-Hexa-1,5-diyn-3-ene for the Initial and Final Points of Each Step Identified on the Reaction Path (First Column Is (*Z*)-Hexa-1,5-diyn-3-ene, Step III Coincides with the TS, and the Last Column Is *p*-Benzyne)

step	I		II		III (TS)	IV		V	
$V(C_1,C_2)$	5.40	5.36	4.74	4.28	4.28	4.16	3.62	3.60	2.84
$V(C_2,C_3)$	2.33	2.39	2.39	2.39	2.40	2.41	2.48	2.49	2.84
$V_{1,2}(C_3,C_4)$	1.69	1.65	1.65	1.6	3.16	3.14	3.07	3.05	2.58
	1.69	1.65	1.65	1.6					
$V(C_5,C_4)$	2.33	2.39	2.38	2.39	2.40	2.41	2.48	2.49	2.84
$V(C_6,C_5)$	5.40	5.36	4.74	4.28	4.28	4.16	3.62	3.60	2.84
$V(C_2)$			0.62	1.16	1.17	1.18	1.20	1.22	1.24
$V(C_5)$			0.62	1.16	1.17	1.18	1.20	1.22	1.24
$V(C_1)$						0.12	0.63		
$V(C_6)$						0.12	0.63		
$V(C_1,C_6)$								1.31	2.58
$V(H_7,C_1)$	2.23	2.26	2.27	2.21	2.19	2.18	2.15	2.15	2.12
$V(H_8,C_3)$	2.12	2.09	2.09	2.11	2.11	2.11	2.11	2.11	2.12

TABLE 2: Rx,[a] Energy,[b] Increments of Energy within Each Step,[c] and Geometrical Parameters[d,e] Calculated for the Initial and Final Points of Each Step Identified on the Reaction Path Using the ELF Analysis (First Column Is (*Z*)-Hexa-1,5-diyn-3-ene, Step III Coincides with the TS, and the Last Column Is *p*-Benzyne)

step	I		II		III (TS)	IV		V	
Rx[a]	reactive	−2.27	−2.23	−0.04	0.00	0.04	0.75	0.79	product
E[b]	−230.8802	−230.8449	−230.8446	−230.8308	−230.8308	−230.8309	−230.8376	−230.8383	−230.8687
ΔE[c]	0	+22.13	0	+8.65	0.06	0	−4.23	0	−19.05
rC_1-C_2[d]	1.211	1.225	1.226	1.261	1.265	1.269	1.290	1.292	1.346
rC_2-C_3	1.417	1.413	1.413	1.397	1.395	1.393	1.384	1.383	1.346
rC_3-C_4	1.355	1.375	1.376	1.399	1.401	1.404	1.418	1.419	1.480
rC_2-C_5	2.996	2.706	2.707	2.741	2.742	2.743	2.746	2.746	2.727
rC_1-C_6	4.482	2.484	2.475	2.012	1.981	1.951	1.806	1.798	1.480
rC_1-H_7	1.066	1.067	1.067	1.073	1.074	1.074	1.078	1.079	1.084
rC_3-H_8	1.088	1.085	1.085	1.085	1.085	1.085	1.085	1.085	1.084
$aC_1-C_2-C_3$[e]	177.5	146.7	146.5	134.5	133.8	133.1	130.0	129.8	124.8
$aC_2-C_3-C_4$	125.4	118.1	118.1	118.7	118.7	118.7	118.7	118.6	117.6
$aH_7-C_1-C_2$	178.6	166.6	166.4	149.1	147.8	146.4	140.0	139.6	127.4
$aH_8-C_3-C_4$	118.0	119.9	119.8	118.2	118.1	117.9	117.2	117.2	114.9

[a] In $amu^{1/2}$ bohr. [b] In au. [c] In kcal/mol. [d] Distances in angstroms. [e] Angles in degrees.

exponent equal to null. Along the reaction path, the chemical system goes from a given structural stability domain or step to another by means of bifurcation catastrophes occurring at the turning points. Each catastrophe transforms the overall topology in such a way that the Poincaré−Hopf relation is fulfilled. The evolution of ELF basin populations along the reaction path provides insight to understand the complex and often subtle changes in the electronic structure during chemical reactions. Three types of bifurcation catastrophes have been found in the study of chemical reactivity: (i) the fold catastrophe, corresponding to the creation or to the annihilation of two critical points of different parity; for example, a wandering point gives rise to an attractor (index 0) and a saddle point of index 1; (ii) the cusp catastrophe, which transforms one critical point into three (and vice versa) such as in the formation or the breaking of a covalent bond; and (iii) the elliptic umbilicus in which the index of a critical point changes by two.

The topological analysis of ELF allows the identification of the electron pairs in the molecule, but there is no a direct relationship to a "classic" and useful concept such as aromaticity, which is one important aspect in the Bergman reaction. Hence, we have employed a new tool that enables us to perform the topological analysis of a separation of ELF in ELF_σ and ELF_π contributions, considering exclusively the in-plane and out-of-plane orbitals. Note that there are five filled π molecular orbitals in the analyzed system, but just three π orbitals contain the information about the six out-of-plane electrons that generate the π-aromaticity of *p*-benzyne. Thus, only these three orbitals are considered to construct ELF_π, while the others are employed for ELF_σ. We employ the value of the $ELF_{\sigma,\pi}$ for which there is a reduction of the entire $ELF_{\sigma,\pi}$ domain into smaller ones as a direct measure of aromaticity of the σ,π electronic cloud.

Results and Discussion

In Table 1, the integrated electronic population of ELF valence basins at the initial and final points of each step is presented. Also, reaction coordinate (Rx), energies, and geometrical parameters of the same points are shown in Table 2, to obtain a global correspondence between changes in the electronic structure, energy, and geometrical parameters. The reaction path calculated at (R/BS-U) B3LYP/6-31G(d) is presented in Figure 1, where the steps obtained by ELF analysis are specified. The development of the aromaticity along the IRC path is assessed in Figure 2. In Figure 3, a representation of the ELF basins is shown to help visualize the most relevant steps along the IRC path.

An analysis of the results displayed in Figure 3 shows that the reactive (see Figure 3a), (*Z*)-hexa-1,5-diyn-3-ene, presents six core basins on carbon atoms $C(C_{1-6})$, which characterize the core electron pairs with an integrated basin population of 2.07e each. The integrated electron population is slightly larger than the expected value of 2.00e due to the weaker effective potential felt by the valence electrons.[9] These basins do not interact with the valence basins and will remain unaltered along the IRC. There are two pairs of C−H bonds, represented by disynaptic basins $V(H_{7,10},C_{1,6})$ and $V(H_{8,9},C_{3,4})$, with populations of 2.23e and 2.12e, respectively. An integrated population larger than 2.00e for a hydrogenated basin is explained by a small contribution of a resonance structure involving a lone pair on the carbon atom. Because the averaged ELF basin population

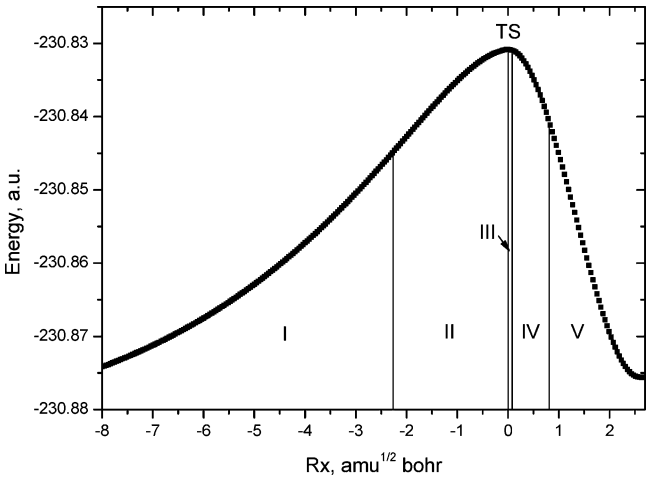

Figure 1. Energy profile calculated by means of the IRC method for the Bergman cyclization of (*Z*)-hexa-1,5-diyn-3-ene to yield *p*-benzyne. There are, in total, 266 points calculated with a step size of 0.04 [amu$^{1/2}$ bohr].

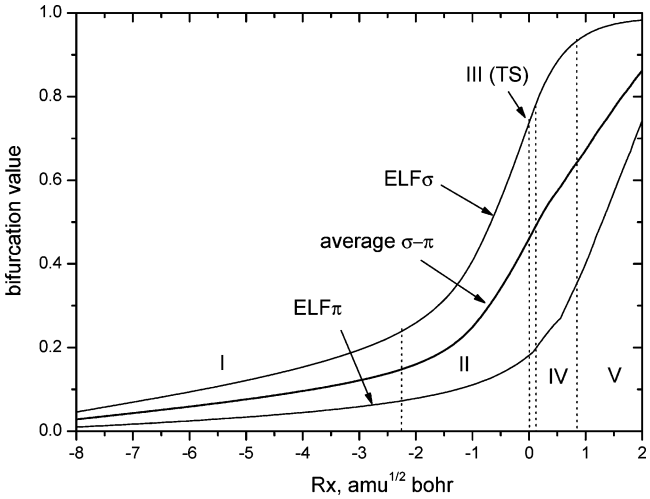

Figure 2. Values of the ELF$_\sigma$, ELF$_\pi$, and aromaticity index (average $\sigma-\pi$) at the bifurcation point along the IRC path.

is interpreted in terms of a superposition of weighted resonance structure contributions, then the bond population is twice the topologically defined Lewis indexes. The reactant presents three types of disynaptic C,C basins: V($C_{2,5}$,$C_{3,4}$) with a population of 2.33e, two degenerate $V_{1,2}$(C_3,C_4) disynaptic basins that integrate to 3.38e, and V($C_{1,6}$,$C_{2,5}$) with a population of 5.40e.

During the first step, there are just small variations in the population of ELF basins, but the geometry changes strongly (see Tables 1 and 2); the distance rC$_1-$C$_6$ and the angle aC$_{1,6}-$C$_{2,5}-$C$_{3,4}$ decrease from 4.482 to 2.484 Å and from 177.5° to 146.7°, respectively. It is interesting to note that this step is the most costly in terms of energy (22.13 kcal/mol) and a destabilization of the reactive by pulling together C_1 and C_6 atoms can be a suitable model for this step of the reaction, as it is shown by Kraka and Cremer[37] using ab initio calculations. Our results show that in this step, the acetylene bonds are bent but not broken, in agreement with the observation of Galraith et al. that changes in geometry are not synchronized with changes in the electronic structure.[48] Also, Alabugin et al.,[54] using NBO π-bond orders, show there is no breaking of acetylene bonds at the first stage of the reaction.

The relevance of electron repulsion between acetylenic groups has been postulated for a long time,[35] but its role has not been quantified. To assess the influence of this factor together with

SCHEME 2: Bending of the $C_1-C_2-C_3$ Angle (α) in 1-Buten-3-yne

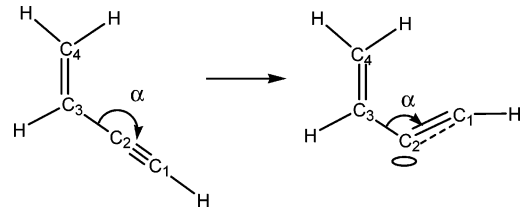

the bending of the $C_{1,6}-C_{2,5}-C_{3,4}$ structure, we will scan the bending of the same unit in 1-buten-3-yne molecule reoptimized for each fixed value of α from 190° to 120° in steps of 5°, at the B3LYP/6-31G(d) calculation level.

According to Figure 4 (point 1), the energy cost of bending the $C_1-C_2-C_3$ unit in 1-buten-3-yne (Scheme 2) to 146.7°, which corresponds to the value of α at the last point of step I for the (*Z*)-hexa-1,5-diyne-3-ene cyclization, is 8.8 kcal/mol. The increment of energy of the first step in the (*Z*)-hexa-1,5-diyne-3-ene cyclization is 22.13 kcal/mol, so the electrostatic repulsion energy should be around 5 kcal/mol, assuming that the bending of the two acetylene units is independent (bending energy = 17.6 kcal/mol). Moreover, an ELF analysis of the scan over α in 1-buten-3-yne reveals that V(C_2) appears at a bending angle of $\alpha \approx 140°$ (Figure 4, point 2). Thus, the two destabilizing factors play a cooperative role in the (*Z*)-hexa-1,5-diyne-3-ene cyclization. Initially, the bending of the $C_{1,6}-C_{2,5}-C_{3,4}$ per se will increase the energy and creates the V(C_2) and V(C_5) basins, and the closed-shell repulsion with the other acetylene group enhances the process of biradicaloid formation.

The second step (II) starts at Rx = −2.23 amu$^{1/2}$ bohr and lasts for 56 points on the IRC path, increasing the energy in 8.65 kcal/mol. Two new monosynaptic basins V(C_2) and V(C_5) are formed by a fold-type catastrophe (see Figure 3b). The bending distortion of the $C_{1,6}-C_{2,5}-C_{3,4}$ angle that occurred along the first step originated vacancies on C_2 and C_5 atoms, and the repulsive interaction between the largely populated V(C_1,C_2) and V(C_6,C_5) basins pushes density away of the interacting region to the backside of C_2 and C_5. Thus, the system finds a natural way to attemperate the closed-shell interaction between terminal acetylene groups by transferring electron density from mutually repelling basins, V(C_1,C_2) and V(C_6,C_5), to the new basins V(C_2) and V(C_5), enhancing the biradicaloid character of the moiety. In this step, an electron pair moves from V(C_1,C_2) (and V(C_6,C_5)) to the C_2 (and C_5) atom carrying only a small amount of electron density, and it does not imply a total breaking of the in-plane π bonds. Along this step, there is a charge transfer of about 0.60e from V($C_{1,6}$,$C_{2,5}$) basins to V(C_2) and V(C_5) basins, while energy rises 8.70 kcal/mol. Looking at Table 2, changes of the electronic structure are reflected in changes of the geometry; there is a noticeable shortening of rC$_1-$C$_6$ (from 2.475 to 2.012 Å), rC$_1-$C$_2$ increases from 1.226 to 1.261 Å, while rC$_1-$C$_6$ decreases from 2.475 to 2.012 Å.

The turning point that defines the third step (III) coincides with the TS. At this point, the degenerate basins $V_{1,2}$(C_3,C_4) corresponding to the double bond C_3-C_4 are transformed into one single basin, V(C_3,C_4), by a cusp-type catastrophe. This step takes only one point on the IRC path and points out the beginning of the participation of the double bond C_3-C_4 in the reaction. The distance rC$_1-$C$_6$ is 1.981 Å, but there is no evidence of bonding between the atoms. Note that the populations of V($C_{1,6}$,$C_{2,5}$) are 4.28e each; the repulsive interaction between these basins is increased due to their proximity. It is

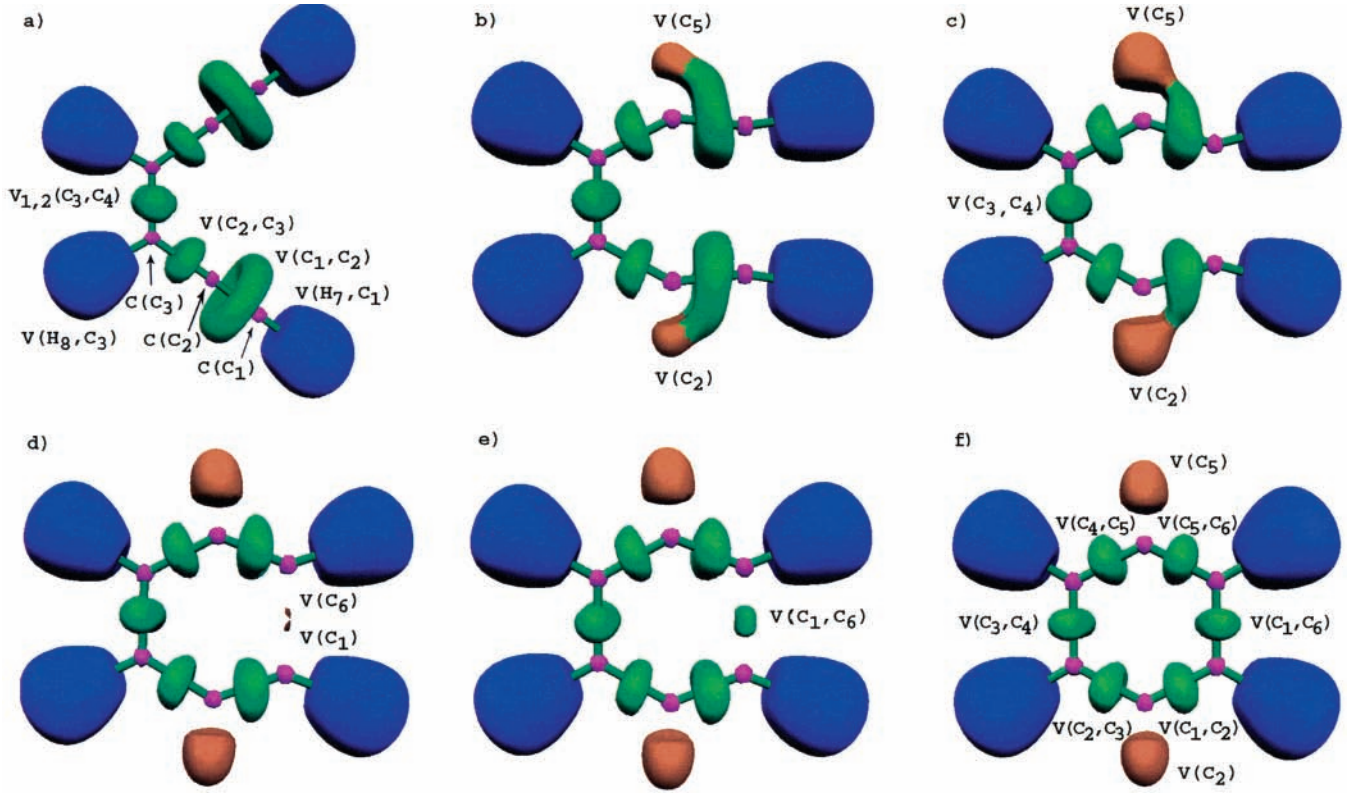

Figure 3. Snapshots of ELF localization domains ($\eta = 0.80$ isosurface) for (a) reactant, (*Z*)-hexa-1,5-diyn-3-ene, (b) step II turning point, (c) step III (same as TS), (d) step IV turning point, (e) step V turning point, and (f) product, *p*-benzyne. Basin color legend: red for core, blue for hydrogenated, orange for monosynaptic, and green for disynaptic.

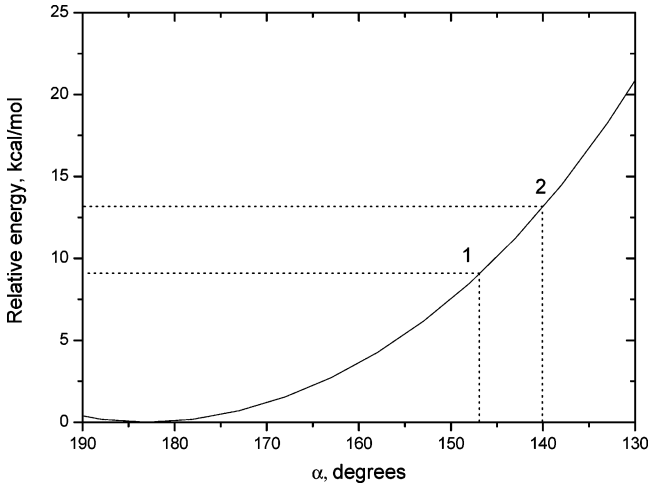

Figure 4. Relative energy (in kcal/mol) versus scan of the $C_1-C_2-C_3$ bending angle (α) for 1-buten-3-yne.

remarkable that the system possesses a large biradicaloid character (population of the basins $V(C_2)$ and $V(C_5)$ is 1.17e), but it is a closed-shell system. Figure 3 reveals that in the TS there is a large delocalization of the σ electronic system ($ELF_\sigma = 0.72$) and no trace of π-aromaticity ($ELF_\pi = 0.16$). These results on σ,π-aromaticity are in good agreement with previous studies using different methodologies (VB resonance energies and NICS).[48]

One point after the TS, the RB3LYP description becomes unstable and the IRC is then calculated using BS-UB3LYP. Note that the change from closed-shell to open-shell calculation does not change the trend of the ELF basin populations.

The next step (IV) ranges from Rx = +0.04 to +0.75 amu$^{1/2}$ bohr and energy decreases in 4.23 kcal/mol. Two new monosynaptic basins are created on C_1 and C_6 atoms by means of a fold-type catastrophe (see Figure 3d). Inspection of the populations reveals that the electron density of the new basins is been transferred from $V(C_{1,6},C_{2,5})$ basins. Formally, we can say that the in-plane π-bond has been definitively broken. This step is the prelude of the formation of a disynaptic basin $V(C_1,C_6)$. Along this step, ELF_σ increases from 0.76 to 0.93, while ELF_π goes from 0.18 to 0.33, revealing the existence of σ-aromaticity, whereas there is still no π-aromaticity of the out-of-plane electron cloud.

SCHEME 3: Schematic Representation of the Reaction Mechanism for the Bergman Cyclization of (*Z*)-Hexa-1,5-diyne-3-ene from the Perspective of the ELF Analysis

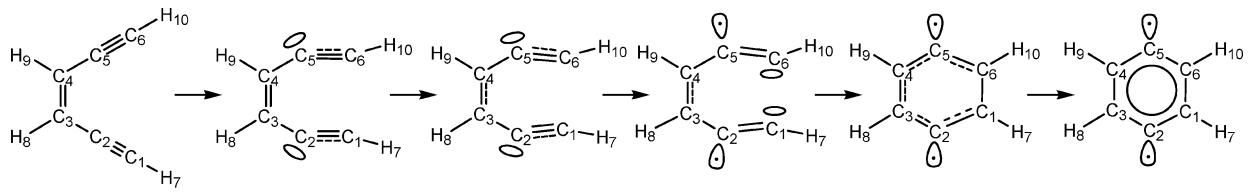

The last step (V) of the mechanism is the closure of the ring by formation of the C_1-C_6 covalent bond. Monosynaptic basins $V(C_1)$ and $V(C_6)$ evolve into a disynaptic basin $V(C_1,C_6)$, by a cusp-type catastrophe (see Figure 3e). The basin possesses an initial population of 1.31e, which increases gradually along the step reaching a final value of 2.58e at *p*-benzyne. The charge density of the new bond is being transferred from $V(C_{1,6},C_{2,5})$ basins. The unpaired electrons at $V(C_2)$ and $V(C_5)$ increase the population slightly up to 1.24e. Along this step, the molecule is stabilized in 19.05 kcal/mol, and the main geometrical change is the shortening of rC_1-C_6. In this region, the bifurcation value of the ELF_π basin goes up from 0.35 to 0.83, showing that the increment of the aromaticity of the π system occurs exclusively in the very last stage of the reaction, after the bond C_1-C_6 is definitively formed. The degree of π-aromaticity of the *p*-benzyne biradical (0.83) is considerable, but it is lower than benzene (0.91).[29] In summary, the reaction mechanism interpreted by the ELF can be represented in Scheme 3.

Conclusions

We have employed the electron localization function (ELF), catastrophe theory, and the value of $ELF_{\sigma,\pi}$ bifurcation, as a measure of the aromaticity, to obtain a novel perspective to understand the electronic rearrangements of the Bergman cyclization. It is the purpose of this paper to point out that the topological analysis of ELF can be used to complement the molecular orbital or valence bond-based methods. Our methodology provides a rather suitable tool for the study of chemical reactivity because it accounts consistently energetic, geometrical, and electronic changes along an accurate IRC path and classifies chemical events (bond breaking/forming processes, presence of diradicaloids or lone pairs, aromaticity of $\sigma-\pi$ electronic systems) in a clear and rigorous way. In this sense, the concepts employed in the present work have found both physical meaning (ELF) and mathematical foundation (catastrophe theory). Therefore, relevant results obtained in previous theoretical studies were discussed, compared, and analyzed within the present framework. The results can be summarized as follows:

(a) The reaction can be described in five domains of structural stability of the ELF characterized by four catastrophes (fold-cusp-fold-cusp). These domains are associated with a sequence of elementary chemical steps.

(b) Our methodology gives a reasonable and consistent analysis in ELF terms for stabilizing/destabilizing factors along the IRC path. The order of appearance of these effects can be established as: (1) mechanical bending deformation of the $C_{1,6}-C_{2,5}-C_{3,4}$ moieties with concomitant repulsion between closed-shell acetylene groups, (2) formation of biradicaloids on C_2 and C_5 atoms, (3) the approximation of C_1 and C_6 atoms leading to aromaticity of the σ electronic system, (4) ring closure by formation of the C_1-C_6 covalent bond, and, finally, (5) development of π-aromaticity, which becomes maximum for *p*-benzyne.

(c) The value of the ELF at the point where there is a reduction of the entire ELF_π is employed to assess consistently the degree of aromaticity. The TS presents a moderate aromatic character provided exclusively by the delocalization of the in-plane electronic system ($ELF_\sigma = 0.71$, $ELF_\pi = 0.16$). The π-aromaticity comes into consideration at the final stage of the reaction, once the ring is formed.

Acknowledgment. J.C.S. thanks the Fundació Bancaixa-Universitat Jaume I for the financial support of a research stay at Universitat Jaume I. This work was supported by Universitat Jaume I-Fundació Bancaixa, project P1B99-02, Ministerio de Ciencia y Tecnología, project BQU2003-04168-C03-03, and Universidad Técnica Federico Santa Maria grant UTFSM 130423, MIDEPLAN, through Millennium Nucleus for Applied Quantum Mechanics and Computational Chemistry P02-004-F and FONDECYT Grants 1010649 and 1030548. We thank the Servei d'Informatica, Universitat Jaume I, for generous allotment of computer time.

References and Notes

(1) Becke, A. D.; Edgecombe, K. E. *J. Chem. Phys.* **1990**, *92*, 5397.
(2) McWeeny, R. *Rev. Mod. Phys.* **1960**, *32*, 335.
(3) McWeeny, R. *Methods of Molecular Quantum Mechanics*, 2nd ed.; Academic Press: New York, 1989.
(4) Silvi, B.; Savin, A. *Nature* **1994**, *371*, 683.
(5) Savin, A.; Becke, A. D.; Flad, J.; Nesper, R.; Preuss, H.; Vonschnering, H. G. *Angew. Chem., Int. Ed. Engl.* **1991**, *103*, 421.
(6) Savin, A.; Jepsen, O.; Flad, J.; Andersen, O. K.; Preuss, H.; Vonschnering, H. G. *Angew. Chem., Int. Ed. Engl.* **1992**, *104*, 186.
(7) Savin, A.; Silvi, B.; Colonna, F. *Can. J. Chem.* **1996**, *74*, 1088.
(8) Kohout, M.; Savin, A. *Int. J. Quantum Chem.* **1996**, *60*, 875.
(9) Noury, S.; Colonna, F.; Savin, A.; Silvi, B. *J. Mol. Struct.* **1998**, *450*, 59.
(10) Silvi, B. *J. Phys. Chem. A* **2003**, *107*, 3081.
(11) Savin, A.; Nesper, R.; Wengert, S.; Fassler, T. F. *Angew. Chem., Int. Ed. Engl.* **1997**, *109*, 1892.
(12) (a) Llusar, R.; Beltran, A.; Andres, J.; Noury, S.; Silvi, B. *J. Comput. Chem.* **1999**, *20*, 1517. (b) Berski, S.; Gutsev, G. L.; Mochena, M. D.; Andres, J. *J. Phys. Chem. A* **2004**, *108*, 6025.
(13) Fuster, F.; Sevin, A.; Silvi, B. *J. Phys. Chem. A* **2000**, *104*, 852.
(14) Fuster, F.; Sevin, A.; Silvi, B. *J. Comput. Chem.* **2000**, *21*, 509.
(15) Fuster, F.; Silvi, B. *Chem. Phys.* **2000**, *252*, 279.
(16) Oliva, M.; Safont, V. S.; Andres, J.; Tapia, O. *Chem. Phys. Lett.* **2001**, *340*, 391.
(17) Chamorro, E.; Santos, J. C.; Gomez, B.; Contreras, R.; Fuentealba, P. *J. Phys. Chem. A* **2002**, *106*, 11533.
(18) Chamorro, E.; Toro-Labbe, A.; Fuentealba, P. *J. Phys. Chem. A* **2002**, *106*, 3891.
(19) Chesnut, D. B. *J. Phys. Chem. A* **2003**, *107*, 4307.
(20) Michelini, M. D.; Sicilia, E.; Russo, N.; Alikhani, M. E.; Silvi, B. *J. Phys. Chem. A* **2003**, *107*, 4862.
(21) Krokidis, X.; Noury, S.; Silvi, B. *J. Phys. Chem. A* **1997**, *101*, 7277.
(22) Krokidis, X.; Silvi, B.; Alikhani, M. E. *Chem. Phys. Lett.* **1998**, *292*, 35.
(23) Krokidis, X.; Goncalves, V.; Savin, A. *J. Phys. Chem. A* **1998**, *102*, 5065.
(24) Krokidis, X.; Vuilleumier, R.; Borgis, D.; Silvi, B. *Mol. Phys.* **1999**, *96*, 265.
(25) Chamorro, E.; Santos, J. C.; Gomez, B.; Contreras, R.; Fuentealba, P. *J. Chem. Phys.* **2001**, *114*, 23.
(26) Berski, S.; Andres, J.; Silvi, B.; Domingo, L. R. *J. Phys. Chem. A* **2003**, *107*, 6014.
(27) Polo, V.; Andres, J.; Castillo, R.; Berski, S.; Silvi, B. *Chem.-Eur. J.* **2004**, *10*, 5165.
(28) Thom, R. *Structural Stability and Morphogenesis: An Outline of a General Theory of Models*; Benjamin: Reading, 1975. Poston, T.; Stewart, L. *Catastrophe Theory and its Applications*; Dover Publications: Mineola, NY, 1996.
(29) Santos, J. C.; Tiznado, W.; Contreras, R.; Fuentealba, P. *J. Chem. Phys.* **2004**, *120*, 1670.
(30) Santos, J. C.; Andres, J.; Aizman, A.; Fuentealba, P. *J. Chem. Theory Comput.* **2005**, in press.
(31) Melin, J.; Fuentealba, P. *Int. J. Quantum Chem.* **2003**, *92*, 381.
(32) (a) Jones, R. R.; Bergman, R. G. *J. Am. Chem. Soc.* **1972**, *94*, 660. (b) Bergman, R. G. *Acc. Chem. Res.* **1973**, *6*, 25.
(33) Nicolaou, K. C.; Dai, W. M. *Angew. Chem., Int. Ed. Engl.* **1991**, *30*, 1387. Nicolaou, K. C.; Smith, A. L. *Acc. Chem. Res.* **1992**, *25*, 497. Casazza, A. M.; Kelly, S. L. *Enediyne Antibiotics as Antitumor Agents*; Marcel Dekker: New York, 1995; Vol. 14.
(34) Grissom, J. W.; Gunawardena, G. U.; Klingberg, D.; Huang, D. H. *Tetrahedron* **1996**, *52*, 6453.
(35) Koga, N.; Morokuma, K. *J. Am. Chem. Soc.* **1991**, *113*, 1907.
(36) Wierschke, S. G.; Nash, J. J.; Squires, R. R. *J. Am. Chem. Soc.* **1993**, *115*, 11958.
(37) Kraka, E.; Cremer, D. *J. Am. Chem. Soc.* **1994**, *116*, 4929.
(38) Lindh, R.; Persson, B. J. *J. Am. Chem. Soc.* **1994**, *116*, 4963.
(39) Logan, C. F.; Chen, P. *J. Am. Chem. Soc.* **1996**, *118*, 2113.
(40) Cramer, C. J.; Nash, J. J.; Squires, R. R. *Chem. Phys. Lett.* **1997**, *277*, 311.
(41) Schreiner, P. R. *J. Am. Chem. Soc.* **1998**, *120*, 4184.

(42) Chen, W. C.; Chang, N. Y.; Yu, C. H. *J. Phys. Chem. A* **1998**, *102*, 2584.
(43) Cramer, C. J. *J. Am. Chem. Soc.* **1998**, *120*, 6261.
(44) Lindh, R.; Bernhardsson, A.; Schutz, M. *J. Phys. Chem. A* **1999**, *103*, 9913.
(45) Koseki, S.; Fujimura, Y.; Hirama, M. *J. Phys. Chem. A* **1999**, *103*, 7672.
(46) Haberhauer, G.; Gleiter, R. *J. Am. Chem. Soc.* **1999**, *121*, 4664.
(47) Gräfenstein, J.; Hjerpe, A. M.; Kraka, E.; Cremer, D. *J. Phys. Chem. A* **2000**, *104*, 1748.
(48) Galbraith, J. M.; Schreiner, P. R.; Harris, N.; Wei, W.; Wittkopp, A.; Shaik, S. *Chem.-Eur. J.* **2000**, *6*, 1446.
(49) Prall, M.; Wittkopp, A.; Schreiner, P. R. *J. Phys. Chem. A* **2001**, *105*, 9265.
(50) Jones, G. B.; Warner, P. M. *J. Am. Chem. Soc.* **2001**, *123*, 2134.
(51) Clark, A. E.; Davidson, E. R.; Zaleski, J. M. *J. Am. Chem. Soc.* **2001**, *123*, 2650.
(52) Kraka, E.; Cremer, D. *J. Comput. Chem.* **2001**, *22*, 216.
(53) Stahl, F.; Moran, D.; Schleyer, P. V.; Prall, M.; Schreiner, P. R. *J. Org. Chem.* **2002**, *67*, 1453.
(54) Alabugin, I. V.; Manoharan, M. *J. Phys. Chem. A* **2003**, *107*, 3363.
(55) Nicolaou, K. C.; Ogawa, Y.; Zuccarello, G.; Kataoka, H. *J. Am. Chem. Soc.* **1988**, *110*, 7247.
(56) Becke, A. D. *Phys. Rev. A* **1988**, *38*, 3098.
(57) Becke, A. D. *J. Chem. Phys.* **1993**, *98*, 1372.
(58) Lee, C. T.; Yang, W. T.; Parr, R. G. *Phys. Rev. B* **1988**, *37*, 785.
(59) Hariharan, P. C.; Pople, J. A. *Theor. Chim. Acta* **1973**, *28*, 213.
(60) Frisch, M. J.; Trucks, G. W.; Schlegel, H. B.; Scuseria, G. E.; Robb, M. A.; Cheeseman, J. R.; Zakrzewski, V. G.; Montgomery, J. A.; Stratmann, R. E., Jr.; Burant, J. C.; Dapprich, S.; Millam, J. M.; Daniels, A. D.; Kudin, K. N.; Strain, M. C.; Farkas, O.; Tomasi, J.; Barone, V.; Cossi, M.; Cammi, R.; Mennucci, B.; Pomelli, C.; Adamo, C.; Clifford, S.; Ochterski, J.; Petersson, G. A.; Ayala, P. Y.; Cui, Q.; Morokuma, K.; Malick, D. K.; Rabuck, A. D.; Raghavachari, K.; Foresman, J. B.; Cioslowski, J.; Ortiz, J. V.; Baboul, A. G.; Stefanov, B. B.; Liu, G.; Liashenko, A.; Piskorz, P.; Komaromi, I.; Gomperts, R.; Martin, R. L.; Fox, D. J.; Keith, T.; Al-Laham, M. A.; Peng, C. Y.; Nanayakkara, A.; Challacombe, M.; Gill, P. M. W.; Johnson, B.; Chen, W.; Wong, M. W.; Andres, J. L.; Gonzalez, C.; Head-Gordon, M.; Replogle, E. S.; Pople, J. A. *Gaussian 98*, revision A.9; Gaussian, Inc.: Pittsburgh, PA, 1998.
(61) Fukui, K. *J. Phys. Chem.* **1970**, *74*, 4161.
(62) Fukui, K. *Acc. Chem. Res.* **1981**, *14*, 363.
(63) Gonzalez, C.; Schlegel, H. B. *J. Phys. Chem.* **1990**, *94*, 5523.
(64) Bauernschmitt, R.; Ahlrichs, R. *J. Chem. Phys.* **1996**, *104*, 9047.
(65) (a) Cremer, D.; Filatov, M.; Polo, V.; Kraka, E.; Shaik, S. *Int. J. Mol. Sci.* **2002**, *3*, 604. (b) Polo, V.; Kraka, E.; Cremer, D. *Theor. Chem. Acc.* **2002**, *107*, 291.
(66) Noury, S.; Krokidis, X.; Fuster, F.; Silvi, B. TopMoD Package; Universite Pierre et Marie Curie, 1997.
(67) Flükiger, P.; Lüthi, H. P.; Portmann, S.; Weber, J. MOLEKEL 4.0; J. Swiss Center for Scientific Computing, Manno, Switzerland, 2000.